Isotopically Selective Infrared Multiphoton Dissociation of 2,3-Dihydropyran

Atsushi Yokoyama,* Keiichi Katsumata,† Hironori Ohba, Hiroshi Akagi, Morihisa Saeki, and Keiichi Yokoyama

Quantum Beam Science Directorate, Japan Atomic Energy Agency, Shirakata 2-4, Tokai-mura, Naka-gun, Ibaraki 319-1195, Japan

Received: February 27, 2008; Revised Manuscript Received: May 7, 2008

Oxygen isotopic selectivity on infrared multiphoton dissociation of 2,3-dihydropyran has been studied by the examination of the effects of excitation frequency, laser fluence, and gas pressure on the dissociation probability of 2,3-dihydropyran and isotopic composition of products. Oxygen-18 was enriched in a dissociation product: 2-propenal. The enrichment factor of ^{18}O and the dissociation probability were measured at a laser frequency between 1033.5 and 1057.3 cm^{-1}, the laser fluence of 2.2−2.3 J/cm^2, and the 2,3-dihydropyran pressure of 0.27 kPa. The dissociation probability decreases as the laser frequency being detuned from the absorption peak of 2,3-dihydropyran around 1081 cm^{-1}. On the other hand, the enrichment factor increases with detuning the frequency. The enrichment factor of ^{18}O increases with increasing the 2,3-dihydropyran pressure at the laser fluence of 2.7 J/cm^2 or less and the laser frequency of 1033.5 cm^{-1}, whereas the yield of 2-propenal decreases with increasing the pressure. A very high enrichment factor of 751 was obtained by the irradiation of 0.53 kPa of 2,3-dihydropyran at 2.1 J/cm^2. Collisional effect of vibrationally excited molecules with ambient molecules on isotopic selectivity is discussed on the basis of a rate equation model including a collisional vibrational de-excitation process.

1. Introduction

Naturally, oxygen consists of three stable isotopes: ^{16}O, ^{17}O, and ^{18}O with the abundance ratios of 0.99759:0.00037:0.00204. The oxygen isotopes are widely used as a tracer such as diagnostic of cancer by positron emission tomography. Laser separation of the oxygen isotopes has been studied by UV dissociation of O_2[1] and D_2CO,[2] by IR−UV dissociation of OCS,[3] and by isotopically selective infrared multiphoton dissociation (IRMPD) of many kinds of molecules: $(CH_3)_2O$,[4–6] $COCl_2$,[7] CF_3CH_2OH,[6] C_4H_8O,[5,6] $(CF_3)_2O$,[6,8] $(C_3H_7)_2O$,[5,6] $C_3H_7OCH_3$,[6] CrO_2F_2,[6] C_4F_9COI,[6] $(C_2H_5)_2O$,[5] $C_4H_9OCH_3$,[5] $C_5H_{10}O$[5] and $(CF_3)_2CO$.[9] The enrichment factor of ^{18}O, which is defined as the ratio of the $[^{18}O]/[^{16}O]$ in dissociation products after single laser pulse irradiation to that in the molecules before irradiation, is low for these molecules except $(C_3H_7)_2O$, the largest value for which was 350.[5] Initial reaction of the saturated ethers is simple bond rupture of C−O bond to produce radicals, and secondary reactions and photo-dissociations of primary products determine final products.[10,11] Therefore, oxygen isotopes distribute in some products. For example, CO, H_2CO, CH_3CHO, and CH_3COCH_3 are produced as oxygen-containing products by the IRMPD of $(C_3H_7)_2O$.[10] Relative yields of these products depend on the laser fluence. The production of more than one oxygen-containing products may complicate a recovery process of the enriched oxygen isotopes in these products and reduce production rate of the enriched oxygen isotopes. Moreover, the production of radicals as primary products is unfavorable to isotope separation in some cases, because isotopic scrambling may occur by radical reactions of the primary products with ambient molecules.

Contrary to the simple bond rupture, a concerted reaction usually produces stable products because bond fission and formation occurs simultaneously. The IRMPD of 2,3-dihydropyran (C_5H_8O) dissociates concertedly and produces two stable molecules: 2-propenal (C_3H_4O) and ethylene (C_2H_4).[12] Therefore, the isotopic scrambling of these products with ambient molecules does not occur. Moreover, the IRMPD occurs at low laser fluence, which is essential for a large amount of production of enriched isotopes.[13] In this paper, enrichment of ^{18}O is studied by the isotopically selective IRMPD of C_5H_8O for the first time.

Collisions of molecules during and after a laser pulse affect not only the dissociation yield but also the enrichment factor. Usually, collisions of vibrationally excited molecules with ambient unexcited molecules cause the decrease in the enrichment factor, because the energy transfer from the excited molecules containing the desired isotope to the unexcited molecules containing other isotopes leads to the dissociation of the latter molecules. However, several exceptions are reported: the IRMPD of $(CH_3)_2O$,[6] Si_2F_6,[13] $(CF_3)_2CO$,[14] CF_3Br,[15,16] and $CHClF_2$.[17] The IRMPD of these molecules shows the increase in the enrichment factor with increasing pressure. Because the dependence of the enrichment factor on pressure is important for large-scale isotope separation, we also examined the pressure effect on the IRMPD of C_5H_8O.

2. Experimental Section

2,3-Dihydropyran, the stated purity being more than 95%, was purchased from Kanto chemical Co. Inc. and used without further purifications except for degassing at 77 K. 2,3-Dihydropyran in a stainless steel cell was irradiated through an NaCl window by a TEA CO_2 laser (Lumonics TEA-841). The cell volume was 44.5 cm^3. The laser beam was focused at the center of the cell by a 60 cm focal length BaF_2 lens. The spot size at the focal point was about 2.2 × 3.1 cm^2. The pulse shape of the laser was a 200 ns spike followed by a few microsecond

* Corresponding author. E-mail: yokoyama.atsushi@jaea.go.jp. FAX: +81-29-282-5768. Phone: +81-29-282-5500.

† Present address: Global Environmental Forum, Onogawa 16-2, Tsukuba-shi, Ibaraki 305-8506, Japan.

10.1021/jp802101h CCC: $40.75
Published on Web 06/26/2008

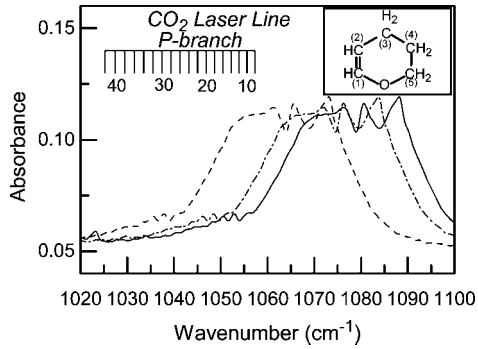

Figure 1. IR absorption spectra of 2,3-dihydropyran. The spectrum for $^{12}C_5H_8{}^{18}O$ (---) is predicted from the calculated isotope shift of 15.1 cm^{-1} and the observed $^{12}C_5H_8{}^{16}O$ spectrum (—). The spectrum for $^{12}C_4{}^{13}CH_8{}^{16}O$ (—•—) is predicted from the isotope shift of 4.4 cm^{-1}, which is calculated in the case that the carbon atom at no. 5 position of the structure shown in the inset is replaced by ^{13}C.

tail. The laser pulse energy measured by a pyroelectric joulemeter (Gentec ED-500) was controlled by inserting a ZnSe beam splitter, CaF_2 plates, or both between the laser and the lens. Irradiated samples were analyzed by a GC/MS instrument (Shimadzu GCMS-QP2010) to determine oxygen isotopic composition in 2-propenal. A 60 m DB-1 widebore capillary column was used as separation column.

3. Results

3.1. Isotope Shift. Figure 1 shows an IR absorption spectrum of C_5H_8O in the frequency range from 1020 to 1100 cm^{-1}. The molecular structure is also shown in the inset. The absorption band in this frequency range is attributed to a C−O stretching mode. Vibrational frequencies of $^{12}C_5H_8{}^{16}O$, $^{12}C_5H_8{}^{18}O$, and $^{12}C_4{}^{13}CH_8{}^{16}O$ were calculated by ab initio molecular orbital calculations at the B3LYP/6-31G(d, p) level of theory using Gaussian 03.[18] The fundamental frequency of $^{12}C_5H_8{}^{18}O$ is calculated to be 15.1 cm^{-1} lower than that of $^{12}C_5H_8{}^{16}O$. Absorption spectrum of $^{12}C_5H_8{}^{18}O$ predicted from the calculated isotope shift is also shown as the dotted line in Figure 1. When one ^{12}C is replaced by ^{13}C, the isotope shift depends on the position of ^{13}C. The largest isotope shift of 4.4 cm^{-1} is obtained when ^{12}C at no. 5 position in the inset of Figure 1 is replaced with ^{13}C. The absorption spectrum of $^{12}C_4{}^{13}CH_8{}^{16}O$ predicted by this calculated isotope shift is also shown as a dotted broken line in Figure 1.

3.2. Determination Procedure of Isotopic Fractions in C_3H_4O. Only two dissociation products, C_3H_4O and C_2H_4, were detected. This implies that the IRMPD of C_5H_8O occurs through a retro-Diels−Alder reaction:[12]

$$C_5H_8O \rightarrow C_3H_4O + C_2H_4 \quad (1)$$

Because C_5H_8O was dissociated by less than 1% in most runs, and because the retention time of C_2H_4 was almost the same as that of nitrogen and oxygen molecules unwillingly mixed with the irradiated samples during the sampling, the isotopic fractions of oxygen and carbon only in C_3H_4O were measured. The isotopic fractions were determined from the signal intensities at $m/e = 55$ ($^{12}C_3H_3{}^{16}O^+$), 56 ($^{12}C_3H_4{}^{16}O^+$ and $^{12}C_2{}^{13}CH_3{}^{16}O^+$), 57 ($^{12}C_2{}^{13}CH_4{}^{16}O^+$ and $^{12}C_3H_3{}^{18}O^+$), and 58 ($^{12}C_3H_4{}^{18}O^+$ and $^{12}C{}^{13}C_2H_4{}^{16}O^+$). Contributions of ^{17}O and D can be neglected because of very low natural abundance: 0.037% for ^{17}O and 0.0148% for D. Because the signal intensity ratio at $m/e = 56$, 55, and 54 is 1.0:0.695:0.015 for natural C_3H_4O under our experimental condition, the production of $C_3H_2O^+$ by electron bombardment of C_3H_4O can also be neglected. Therefore, the isotopic fractions in C_3H_4O can be determined from signal intensities at $m/e = 55$, 56, 57, and 58 as follows:

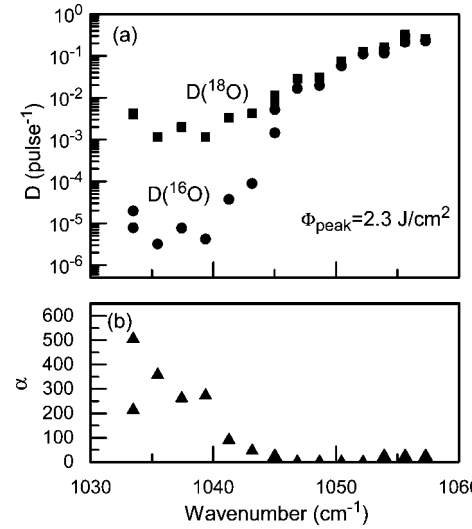

Figure 2. Laser frequency dependence of (a) dissociation probabilities of $C_5H_8{}^{16}O$ D(^{16}O) and $C_5H_8{}^{18}O$ D(^{18}O) and (b) enrichment factor α. The laser fluence at the focus is constant at 2.3 J/cm^2. The C_5H_8O pressure is 0.27 kPa.

$$f(^{13}C) = \frac{[^{13}C]}{[^{12}C] + [^{13}C]} = \frac{x}{1+x} \quad (2a)$$

$$f(^{18}O) = \frac{[^{18}O]}{[^{16}O] + [^{18}O]} = \frac{y}{1+y} \quad (2b)$$

$$x = \frac{[^{13}C]}{[^{12}C]} = \frac{3\{1+\eta(\eta b - a)\} - \sqrt{9\{1+\eta(\eta b - a)\}^2 + 12\eta(\eta b - a)}}{6\eta} \quad (2c)$$

$$y = \frac{[^{18}O]}{[^{16}O]} = (1+3\eta x)b - 3x^2 \quad (2d)$$

where a is the intensity ratio of $m/e = 57$ to $m/e = 56$, b the intensity ratio of $m/e = 58$ to $m/e = 56$, and η the ratio of the $C_3H_3O^+$ yield to the $C_3H_4O^+$ yield produced by the electron bombardment of C_3H_4O. The ratio η can be determined by solving the following equation:

$$3bc\eta^3 - (1+3ac)\eta^2 + 5c\eta - 4c^2 = 0 \quad (3)$$

where c is the intensity ratio of $m/e = 55$ to m/e 56. In the derivation of these equations, ^{13}C is assumed to be statistically distributed among three carbon positions in C_3H_4O.

3.3. Oxygen Isotope Separation. Figure 2a shows CO_2 laser frequency dependence of dissociation probabilities of $C_5H_8{}^{16}O$ and $C_5H_8{}^{18}O$, which are denoted respectively as D(^{16}O) and D(^{18}O). The dissociation probability is defined as the dissociation fraction of the molecules in the irradiation zone of the cell after the irradiation of one laser pulse. Because the laser beam was mildly focused at the center of the cell, the cross sectional areas were 0.22 × 0.31 and 0.30 × 0.38 cm^2 at the center and the windows of the cell, respectively. The irradiation volume V_i (0.77 cm^3) was only 1.7% of the cell volume V_0 (44.5 cm^3).

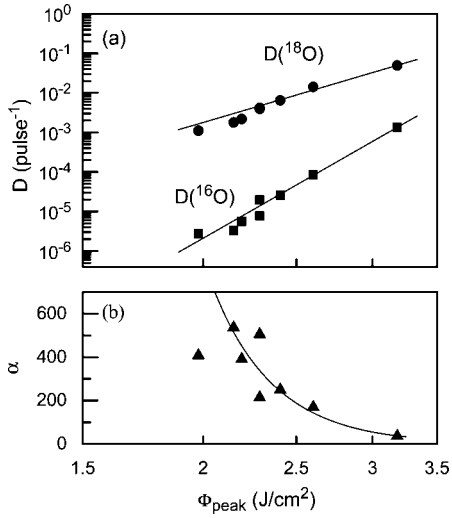

Figure 3. Laser fluence dependence of (a) dissociation rates D and (b) enrichment factor α. The laser frequency is fixed at 1033.5 cm^{-1}, and the C_5H_8O pressure is 0.27 kPa.

The dissociation probability is calculated from the ^{18}O isotopic fraction in C_3H_4O produced after the irradiation of n pulses as follows:

$$D(^{18}O) = -\frac{V_0}{V_i n}\ln\left\{1 - \frac{f(^{18}O)}{0.00204(1 + [C_5H_8O]/[C_3H_4O])}\right\} \quad (4a)$$

$$D(^{16}O) = -\frac{V_0}{V_i n}\ln\left\{1 - \frac{1 - f(^{18}O)}{0.99796(1 + [C_5H_8O]/[C_3H_4O])}\right\} \quad (4b)$$

where the ratio $[C_5H_8O]/[C_3H_4O]$ can be determined from the signal intensity ratio of $C_5H_8O^+$ to $C_3H_4O^+$ with a correction factor determined using standard mixtures of C_5H_8O and C_3H_4O. The data were obtained at peak laser fluence of 2.3 J/cm^2 and C_5H_8O pressure of 0.27 kPa. Both $D(^{18}O)$ and $D(^{16}O)$ decrease with decreasing laser frequency, because the absorption peaks of C_5H_8O locate at higher frequencies. However, the enrichment factor, which is calculated by the ratio $D(^{18}O)/D(^{16}O)$, increases with decreasing laser frequency, as shown in Figure 2b, because the absorption peak for $C_5H_8{}^{18}O$ is 15.1 cm^{-1} lower than that for $C_5H_8{}^{16}O$. $D(^{18}O)$ and $D(^{16}O)$ do not reflect directly the difference between the absorption cross sections of the vibrationally cold $C_5H_8{}^{18}O$ and $C_5H_8{}^{16}O$, because the dissociation probability is determined not only by the cross section of the cold molecules but also by that of the vibrationally hot molecules. For example, $D(^{16}O)$ and $D(^{18}O)$ are comparable at 1050 cm^{-1}, although the absorption cross section of vibrationally cold $C_5H_8{}^{16}O$ molecules is much lower than that of $C_5H_8{}^{18}O$. Because the absorption band of the vibrationally hot molecules shifts to lower frequency, the absorption cross section is expected to increase with increasing the vibrational quantum number when the molecules are irradiated at a low frequency edge of the absorption band of the cold molecules.

The laser fluence dependence of the dissociation probabilities is shown in Figure 3a. The pressure and laser frequency are fixed at 0.27 kPa and 1033.5 cm^{-1}, respectively. The dissociation probabilities are well fitted to the following equation:

$$D = A\Phi_{peak}^{m} \quad (5)$$

where Φ_{peak} is the laser fluence at the focal point. Least squares fittings of the data to eq 5 give $A = (1.2 \pm 0.5) \times 10^{-5}$ $pulse^{-1}$ and $m = 7.2 \pm 0.3$ for $C_5H_8{}^{18}O$, and $A = (1.4 \pm 0.3) \times 10^{-10}$ $pulse^{-1}$ and $m = 13.9 \pm 0.2$ for $C_5H_8{}^{16}O$. Because the m value is smaller for $C_5H_8{}^{18}O$ than for $C_5H_8{}^{16}O$, the enrichment factor increases with decreasing the laser fluence, as shown in Figure 3b. The dissociation probabilities show a high order dependence on fluence. Similar high order dependence was observed in the IRMPD of large molecules such as $C_3H_7OCH_3$,[6] $(C_3H_7)_2O$,[6] and $(CF_3)_2CO$.[9]

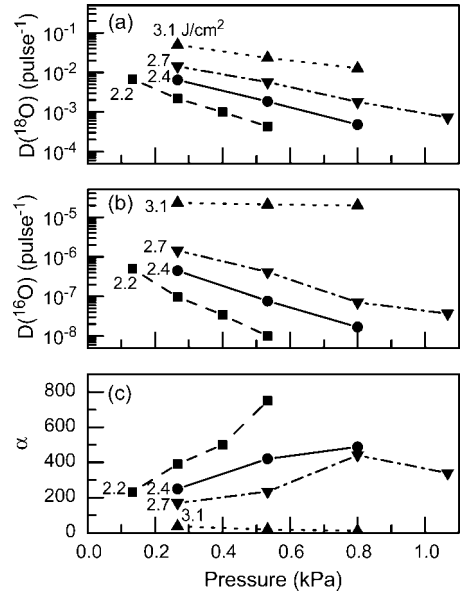

Figure 4. C_5H_8O pressure dependence of (a) dissociation probability of $C_5H_8{}^{18}O$, (b) dissociation probability of $C_5H_8{}^{16}O$, and (c) enrichment factor. The values written at the left side in the figures are the peak laser fluences. The laser frequency is fixed at 1033.5 cm^{-1}.

Pressure dependence of the dissociation probabilities is shown in Figure 4. The pressure dependence was taken at four different fluences ranging from 2.2 to 3.1 J/cm^2. Although $D(^{18}O)$ decreases with the increase in pressure at all laser fluences, $D(^{16}O)$ shows different behavior: i.e., a lower decrease rate is observed when the laser fluence increases, and a slight enhancement with the increase in pressure is observed at 3.1 J/cm^2. Because $D(^{16}O)$ decreases with higher rate than $D(^{18}O)$ at the laser fluence of 2.7 J/cm^2 or less, the enrichment factor increases with the increase in pressure; whereas the enrichment factor decreases with the increase in pressure at 3.1 J/cm.[2] The maximum enrichment factor (751) was observed at the C_5H_8O pressure of 0.53 kPa and the laser fluence of 2.2 J/cm^2.

3.4. Carbon Isotope Separation. Because the signal at $m/e = 57$ comes mainly from $^{12}C_3H_3{}^{18}O^+$ and $^{13}C^{12}C_2H_4{}^{16}O^+$, we need to subtract the contribution of $^{12}C_3H_3{}^{18}O^+$ from the signal intensity at $m/e = 57$ to determine ^{13}C fraction in C_3H_4O. However, the precise determination of the ^{13}C fraction is difficult, because most of the signal comes from $^{12}C_3H_3{}^{18}O^+$ as a result of high enrichment of ^{18}O and low enrichment of ^{13}C. The average ^{13}C fraction is 0.03 ± 0.02 in C_3H_4O produced by the IRMPD of C_5H_8O at the laser frequency of 1033.5 cm^{-1}, the laser fluence range from 2.2 to 3.1 J/cm^2, and C_5H_8O pressure of 0.27 kPa. Because the ^{13}C fraction is consistent with that in natural C_3H_4O (0.032), ^{13}C could not be enriched at this frequency. This is probably due to small isotope shift (0.3−4.4 cm^{-1}) in the C−O stretching mode used for excitation.

3.5. Rate Equation Model. The oxygen enrichment factor was observed to increase with increasing sample pressure as described above. To elucidate the enhancement of the enrichment factor by the increase of the sample pressure, we have

calculated the dissociation probabilities of $C_5H_8{}^{18}O$ and $C_5H_8{}^{16}O$ molecules by a rate equation model.[19] The temporal evolution of ith vibrational level population, N_i, is written by the following differential equation:

$$\frac{dN_i}{dt} = I(t)\{\sigma_{i,i-1}N_{i-1} + \sigma_{i,i+1}N_{i+1} - (\sigma_{i+1,i} + \sigma_{i-1,i})N_i\} + \omega\sum_j P_{ij}N_j - \omega\sum_j P_{ji}N_i - k_iN_i \quad (6)$$

where $I(t)$ is the laser intensity at time t, $\sigma_{i,i\text{-}1}$ the photoabsorption cross section from level $i-1$ to level i, $\sigma_{i,i+1}$ is the induced emission cross section from level $i+1$ to level i, ω is the collision frequency, P_{ij} is the collisional transition probability from level j to level i, and k_i is the unimolecular dissociation rate. The induced emission cross section is related to the photoabsorption cross section by the detail balance: $g_{i+1}\sigma_{i,i+1} = g_i\sigma_{i+1,i}$, where g_i is the degeneracy of level i. The collisional transition probability is calculated here by the step ladder model in which $P_{ij} = 1.0 - P_{ji}$ for $i - j = \langle\Delta E\rangle_d$ and $P_{ij} = 0$ for $i - j \neq \langle\Delta E\rangle_d$, where $\langle\Delta E\rangle_d$ is the average down-energy loss per collision. In simulations for the collisional effect of the IRMPD of small molecules such as CDF_3[20] and $CDCl_3$,[21] an extra differential equation for the ground state population was added for modeling the removal of the rotational bottleneck by collision with buffer gases, i.e., a rate equation expressing the rate of filling of the rotational hole in the ground vibrational state by the collision with ambient molecules. However, the rotational bottleneck effect does not occur in the IRMPD of C_5H_8O even at the lowest pressure of 0.13 kPa. This was confirmed by the measurement of $D(^{18}O)$ and $D(^{16}O)$ for the mixture of C_5H_8O (0.13 kPa) and Ar (0.16 kPa) at the laser frequency of 1033.5 cm^{-1} and the laser fluence of 2.0 J/cm^2. By the addition of Ar, $D(^{18}O)$ and $D(^{16}O)$ decreased to 0.34 and 0.22 of those for the neat C_5H_8O, respectively. Usually, the enhancement of the dissociation probability is observed by the addition of an inert gas when the rotational bottleneck occurs, because the depleted population for the rotational states interacting with laser radiation is recovered by the collision of molecules with buffer gases within the laser pulse duration. Therefore, the rate equation simulating the rotational bottleneck effect is not included in this calculation. Although the experiments suggest the contribution of vibrational-to-vibrational (V−V) energy transfer at the highest laser fluence, this collision model treats only vibrational-to-translational (V−T) energy transfer because of the lack of microscopic rate constants for the V−V process contributing to the IRMPD of C_5H_8O. Although the model calculation includes only the V−T process, this calculation is believed to be useful for the qualitative understanding of collisional effect on the enrichment factor.

The collision frequency was calculated by using the collision cross section of 2.176×10^{-15} cm^2, which was determined from Van der Waals constants estimated from the critical temperature and pressure.[22] The unimolecular dissociation rate was calculated by Rice−Ramsperger−Kaasel−Marcus (RRKM) theory.[23] The parameters used in the calculation are listed in Table 1. The parameters were calculated by ab initio molecular orbital calculations at the B3LYP/6-31G(d,p) level of theory. The calculated activation energy is in good agreement of the reported value (196.54 ± 0.33 kJ/mol).[24] The density of vibrational states were calculated by Witten−Rabinovich approximation.[23] External rotational energy at $T = 300$ K was treated as adiabatic.

TABLE 1: Parameters for Calculations of Unimolecular Dissociation Rate

	$^{12}C_5H_8{}^{18}O$		$^{12}C_5H_8{}^{16}O$	
	molecule	TS	molecule	TS
frequency (cm^{-1})*	3087.2	3160.0	3087.2	3160.0
	3066.7	3112.9	3066.7	3112.9
	2991.1	3100.8	2991.1	3100.8
	2976.8	3070.0	2976.8	3070.0
	2938.7	3067.3	2938.7	3067.3
	2928.0	3026.8	2928.0	3026.8
	2898.4	3020.6	2898.5	3020.6
	2891.7	2873.6	2891.7	2873.7
	1657.9	1531.4	1659.2	1542.0
	1458.3	1519.7	1458.7	1521.0
	1443.6	1462.1	1443.8	1463.6
	1432.5	1427.0	1432.6	1427.0
	1381.6	1399.4	1383.5	1402.8
	1350.0	1307.9	1351.1	1322.0
	1324.2	1233.2	1324.3	1234.3
	1302.8	1198.4	1304.8	1198.5
	1251.8	1193.5	1253.6	1193.7
	1222.3	1077.3	1231.5	1077.9
	1204.4	1065.2	1208.0	1068.9
	1164.7	1012.5	1166.3	1013.0
	1064.6	980.5	1065.5	980.6
	1044.3	947.0	1059.4	948.1
	1022.0	933.8	1023.4	933.9
	999.1	912.8	1000.5	914.5
	908.9	876.4	910.8	877.1
	901.6	812.0	906.5	812.0
	865.3	730.7	871.1	731.8
	854.7	669.0	856.8	676.3
	807.2	602.4	814.4	603.1
	734.6	492.1	736.4	495.2
	711.6	401.3	714.3	401.6
	487.6	350.8	490.7	356.5
	468.5	253.2	476.3	256.8
	425.6	229.6	428.2	234.0
	269.5	150.0	269.8	150.8
	171.9		174.5	
moment of inertia	349.391	383.769	349.290	372.222
	394.701	495.499	380.849	491.196
	684.516	767.781	670.704	753.894
E_0 (kJ/mol)		196.6		196.6

* The frequencies predicted at the B3LYP/6-31G(d, p) level are scaled by 0.9608.

Figure 5 shows the calculated dissociation probabilities and the enrichment factors. The absorption cross section from level n to level $n+1$ was calculated by the following functional form:

$$\sigma(n) = \sigma_0(1 + \gamma n) \quad (7)$$

where σ_0 is the absorption cross section from level 0 to 1. The σ_0 values for $C_5H_8{}^{18}O$ and $C_5H_8{}^{16}O$ were determined to be 6.81×10^{-20} and 3.07×10^{-20} cm^2 from the measured and predicted absorption spectra shown in Figure 1, respectively. The γ values were determined to be 0.126 and 0.216 by the fit respectively to the experimental $D(^{18}O)$ and $D(^{16}O)$ values at the laser fluence of 2.2 J/cm^2 and the pressure of 0.13 kPa. The increase of σ in the increase of the vibrational levels is reasonable, because the absorption spectra usually shift to lower frequency with increasing the level and because the excitation frequency is at the low frequency edge of the absorption band of the vibrationally cold molecules. The rate equations were solved by Runge−Kutta method, and time step for the calculation was 1×10^{-4} ns. The pressure dependence of the dissociation rates are well reproduced with the $\langle\Delta E\rangle_d$ value of 4.123 kJ/mol. Figure 6 shows

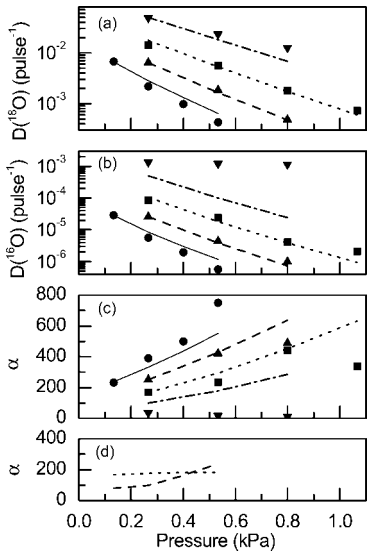

Figure 5. Calculated pressure dependence of dissociation probabilities and enrichment factors: (a) dissociation probabilities of $C_5H_8{}^{18}O$, (b) dissociation probabilities of $C_5H_8{}^{16}O$, (c) enrichment factors, and (d) enrichment factors calculated with the inclusion of collisions only between 0 and 1.5 μs (---) and with the inclusion of collisions only after 1.5 μs (•••) at the laser fluence of 2.2 J/cm^2. In (a), (b) and (c), symbols and lines represent the experimental and calculated results at 2.2 J/cm^2 (● and —), 2.4 J/cm^2 (▲ and ---), 2.7 J/cm^2 (■ and •••), and 3.1 J/cm^2 (▼ and —•—), respectively.

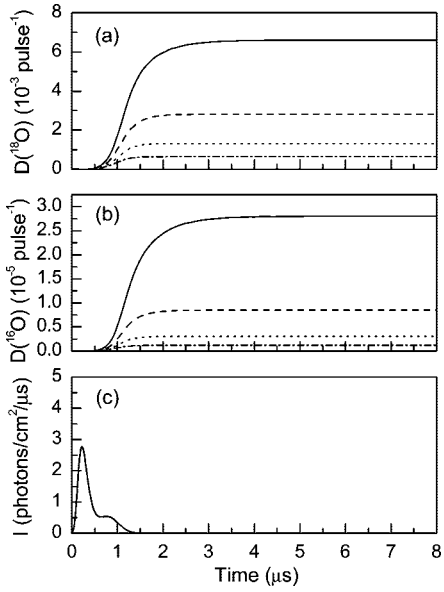

Figure 6. Calculated time-profile of (a) dissociation probability of $C_5H_8{}^{18}O$ and (b) dissociation probability of $C_5H_8{}^{16}O$ at the laser fluence of 2.2 J/cm^2. The sample pressures are 0.13 (—), 0.27 (---), 0.40 (•••), and 0.53 kPa (—•—). The laser pulse intensities *I* used in the calculations are shown in (c).

the time dependence of the dissociation probabilities at the laser fluence of 2.2 J/cm^2 along with the time profile of the laser pulse used in the calculations. The unimolecular dissociation rate for C_5H_8O is low, because C_5H_8O has many fundamental vibrational modes. For example, the rates for $C_5H_8{}^{18}O$ and $C_5H_8{}^{16}O$ at the total pressure of 0.13 kPa are 3693 and 656 s^{-1} at the excess energy above the dissociation threshold of 29 and 19 kJ/mol, which are the average energies of the molecules excited above the dissociation threshold at 1 μs, respectively. Therefore, D(^{18}O) and D(^{16}O) gradually increases after the end of the initial spike of the laser pulse, as shown in Figure 6. Although the unimolecular dissociation rates are very low, the dissociation completes within a few microseconds, and the dissociation probabilities reach to asymptotic values faster with increasing the sample pressure. This is due to the vibrational de-excitation from the vibrational levels above the dissociation threshold to those below the threshold. The calculated time profile of the dissociation probability is supported by the measured time growth of C_3H_4O concentration produced by the IRMPD of 2,3-dihydropyran:[25] the concentration increased gradually from 0.4 to 4.0 μs after the irradiation of laser pulse at the leser fluence of 2.5 J/cm^2.

To examine the collisional effects on the pressure dependence of the enrichment factor within and after the laser pulse, we calculated the dissociation probabilities and the enrichment factors at 2.2 J/cm^2 in two cases: the first case is that no collision occurs after 1.5 μs, and the second case is that no collision occurs between 0 and 1.5 μs. In both cases, collisional de-excitation occurs at another time period than those specified above. The calculated results are shown in Figure 5d as dashed and dotted lines for the first and second cases, respectively. The appreciable enhancement of the enrichment factor by the increase in pressure appears in the first case, whereas the enrichment factor increases only slightly with pressure in the second case.

4. Discussion

4.1. Pressure Effect on the Oxygen Isotopic Selectivity. The enhancement of the enrichment factor with the increase in pressure was observed at the laser fluence of 2.7 J/cm^2 or less. It was also observed in the IRMPD of $(CH_3)_2O$,[6] Si_2F_6[13], $(CF_3)_2CO$,[14] CF_3Br,[15,16] and $CHClF_2$.[17] The IRMPD of CF_3H pre-excited to the second C—H stretch overtone also showed the enhancement of the enrichment factor.[26] In these cases except CF_3H, it was observed when the molecules were excited at the wings of the absorption band as is the case of this study. The two different mechanisms of this enhancement have been proposed: contribution of the removal of rotational bottleneck[16] and contribution of vibrational energy transfer during or after laser pulse.[15,27] However, the first mechanism should not contribute in this case, because the rotational bottleneck effect does not occur in this system as mentioned in section 3.5.

Gauthier et al.[15] explained that the enhancement was due to the different behavior for the competition of the up-pumping through the discrete states to the quasi-continuum states with the vibrational de-excitation; that is, a decrease in the dissociation probability by vibrational de-excitation is smaller for the desired isotopic molecules than for the undesired ones, because the up-pumping rate of the desired isotopic molecules is much higher than that of the undesired isotopic molecules. Bagratashvili et al.[27] discussed on the pressure effect of the enrichment factor for a large molecule like $(CF_3)_2CO$ in the viewpoint of vibrational—vibrational energy transfer between excited and cold molecules after the end of laser pulse in the case of the excitation and dissociation of poor isotopic molecule with high selectivity. They suggested that the difference of the average internal energy between the poor and rich isotopic molecules may affect the extent of the decrease in the dissociation probability: that is, the dissociation probability of the poor isotopic molecules with higher average internal energy is less affected by the vibrational—vibrational exchange with the cold molecules, compared with the dissociation probability of the rich isotopic molecules with lower average internal energy.

The result of the calculation described in section 3.5 clearly indicates the role of collisional de-excitation within and after

TABLE 2: Typical Results for ^{18}O Enrichment

molecule	frequency (cm^{-1})	fluence (J/cm^2)	pressure (kPa)	$D(^{18}O)$ (%)	enrichment factor	ref
C_5H_8O	1033.5	2.1	0.53	0.043	751	this work
	1033.5	2.2	0.27	0.22	391	this work
	1033.5	2.6	0.27	1.4	169	this work
	1033.5	3.2	0.27	5.0	37	this work
$(C_3H_7)_2O$	975.9	1.9	0.016		350	5
	975.9	4.6	0.016	12	26	6
$(CF_3)_2O$	942.4	4	0.067	3	95	6
$C_3H_7OCH_3$	1041.3	3	0.035	3.5	25	6
CF_3CH_2OH	1029.4	1.8	0.027	5	7.2	6
C_4H_8O	1048.7	6.1	0.040	1	1.03	6
	982.1	1.7	0.13		7.4	5
$(CH_3)_2O$	1050.4	3.8	0.67	0.05	16	6
	1057.3	18	0.40		1.9	5
$(CH_3)_3OCH_3$	980.9	2.0	0.13		7.9	5
$C_5H_{10}O$	980.1	1.6	0.13		74	5
$(C_2H_5)_2O$	983.3	1.2	0.13		15	5
CrO_2F_2	944.2	25	0.11		2	6

the laser pulse. As shown in Figure 5d, inclusion of the collisional energy transfer only within the laser pulse leads to the large enhancement of the enrichment factor with increasing pressure, whereas the only slight enhancement occurs in the case that collision occurs only after the laser pulse. Therefore, the collisions within the laser pulse are primarily important for the enhancement of the enrichment factor by the increase in pressure. Compared with the $C_5H_8{}^{18}O$ molecules, the $C_5H_8{}^{16}O$ molecules are severely prevented from exciting above the dissociation threshold by the collisional de-excitation, which competes with photo-excitation during the laser pulse, because the excitation rate for $C_5H_8{}^{16}O$ is lower than that for $C_5H_8{}^{18}O$. Therefore, the fraction of the molecules above the dissociation threshold decreases with increasing pressure with higher rate for $C_5H_8{}^{16}O$ than for $C_5H_8{}^{18}O$ during the laser pulse and consequently the enrichment factor increases with increasing pressure. Collisions after the laser pulse lead to secondary enhancement of the enrichment factor: compared with the $C_5H_8{}^{18}O$ molecules, the $C_5H_8{}^{16}O$ molecules above the dissociation threshold at the end of the laser pulse are more easily de-excited below the dissociation threshold with collisions after the laser pulse, because the average excitation energy is smaller for $C_5H_8{}^{16}O$ than for $C_5H_8{}^{18}O$.

The calculated dissociation probabilities at 2.7 J/cm^2 or less are in good agreement with the observed probabilities. However, the calculation at 3.1 J/cm^2 underestimates largely the probabilities. Especially, the observed $D(^{16}O)$ slightly increases with increasing pressure, whereas the calculated one decreases. This discrepancy may be due to the V−V energy transfer neglected in the calculation:

$$C_5H_8{}^{18}O^* + C_5H_8{}^{16}O \rightarrow C_5H_8{}^{18}O + C_5H_8{}^{16}O^* \quad (8)$$

$$C_5H_8{}^{16}O^* + nh\nu \rightarrow C_2H_4 + C_3H_4{}^{16}O \quad (9)$$

where the asterisk stands for a vibrationally excited states.

Because the fraction of $C_5H_8{}^{18}O^*$ to $C_5H_8{}^{16}O$ is very small at low fluence, the contribution of the above mechanism to $D(^{16}O)$ is considered to be small. However, the mechanism is considered to contribute more largely as the fluence and pressure increase, because the fraction of $C_5H_8{}^{18}O^*$ to $C_5H_8{}^{16}O$ increases and the V−V energy transfer occurs more frequently.

4.2. Comparison of ^{18}O Enrichment with Various Working Molecules. Typical results for ^{18}O enrichment done in this work are shown in Table 2 along with other published works. The highest enrichment factor obtained in this work (751) is more than 2 times as high as that obtained by the IRMPD of $(C_3H_7)_2O$[5] (350), which was the highest one reported before. Although Majima et al.[5] has not reported the dissociation probability for $(C_3H_7)_2O$ at 1.9 J/cm,[2] Laptev et al.[6] noticed that the dissociation probability was less than 0.03% under similar experimental conditions. Therefore, both enrichment factor and dissociation probability are larger for C_5H_8O than for $(C_3H_7)_2O$. Moreover, the IRMPD of $(C_3H_7)_2O$ may complicate the recovery process of the oxygen isotopes, because four oxygen-containing products (CO, H_2CO, CH_3CHO, and CH_3COCH_3) were produced by the IRMPD of $(C_3H_7)_2O$.[10] On the other hand, the enriched oxygen can be easily recovered in the case of the IRMPD of C_5H_8O, because it produces only one oxygen-containing product. Although relatively high enrichment factor and dissociation probability were obtained for $(CF_3)_2O$, the necessity of the relatively high laser fluence and low gas pressure is disadvantageous to the large-scale production of the highly enriched oxygen isotope. The enrichment factor for other molecules is much lower. Therefore, C_5H_8O is best suitable molecule among the studied working molecules for the ^{18}O enrichment by IRMPD.

5. Conclusions

Oxygen isotope separation has been done by the isotopically selective IRMPD of C_5H_8O. The ^{18}O isotope is enriched in C_3H_4O. When the C_5H_8O molecules of 0.27 kPa are excited at the red wing of the absorption band around 1080 cm^{-1}, the enrichment factor increases with decreasing laser frequency and reaches 500 at 1033.5 cm^{-1}. The enrichment factor also increases with the increase in pressure and reaches 751 at 0.53 kPa, which is more than 2 times as large as the highest enrichment factor obtained by the IRMPD of $(C_3H_7)_2O$.[5] This pressure dependence is due to the larger decrease of the dissociation probability with the increase in pressure for $C_5H_8{}^{16}O$ than for $C_5H_8{}^{18}O$ as a result of a smaller photo-absorption cross section. According to the rate equation model including a collisional vibrational de-excitation process, competition of the collisional vibrational de-excitation with the photo-excitation process within the laser pulse is primarily important for the enhancement of the enrichment factor by the increase in pressure, and then the collisional de-excitation of the molecules from the states above the dissociation threshold to the states below the threshold causes secondarily the enhancement after the laser pulse. Although a limited number of the collisional enhancement of the enrichment factor in the IRMPD of molecules has been reported as far as we know, this enhancement process should occur commonly in the isotopically selective IRMPD of large molecules at low laser fluence. Only the stable molecules, C_3H_4O and C_2H_4, are produced primarily by the IRMPD of C_5H_8O as a result of the concerted reaction; the production of only the stable primary products does not cause isotopic scrambling by reactions of the products with remaining C_5H_8O molecules and may be responsible for the observed high enrichment factor together with relatively large isotope shift.

References and Notes

(1) Sander, R. K.; Loree, T. R.; Rockwood, S. D.; Freund, S. M. *Appl. Phys. Lett.* **1977**, *30*, 150.
(2) Marling, J. *J. Chem. Phys.* **1977**, *66*, 4200.
(3) Zittel, P. F.; Darnton, L. A.; Little, D. D. *J. Chem. Phys.* **1983**, *79*, 5991.
(4) Vizhin, V. V.; Molin, Yu. N.; Petrov, A. K.; Sorokin, A. R. *Appl. Phys.* **1978**, *17*, 385.
(5) Majima, T.; Sugita, K.; Arai, S. *Chem. Phys. Lett.* **1989**, *163*, 29.
(6) Laptev, V. B.; Ryabov, E. A.; Tumanova, L. M. *Quantum Electron.* **1995**, *22*, 607.

(7) Abzianidze, T. G.; Baranov, V. Yu.; Bakhtadze, A. B.; Belykh, A. D.; Vetsko, V. M.; Gurashvili, V. A.; Egiazarov, A. S.; Izyumov, S. V.; Kuz'menko, V. A.; Oziashvili, E. D.; Ordzhonikidze, M. O.; Partskhaladze, G. Sh.; Petrov, A. K.; Pis'mennyĭ, V. D.; Putilin, V. M.; Strel'tsov, A. P.; Tevzadse, G. A.; Khomenko, S. V. *Sov. J. Quantum Electron.* **1986**, *16*, 137.

(8) Majima, T.; Igarashi, T.; Arai, S. *Nippon Kagaku Kaishi* **1984**, 1490.

(9) Hackett, P. A.; Willis, C.; Gauthier, M. *J. Chem. Phys.* **1979**, *71*, 2682.

(10) Majima, T.; Ishii, T.; Arai, S. *Bull. Chem. Soc. Jpn.* **1989**, *62*, 1701.

(11) Majima, T.; Ishii, T.; Arai, S. *Bull. Chem. Soc. Jpn.* **1990**, *63*, 728.

(12) Garcia, D.; Keehn, P. M. *J. Am. Chem. Soc.* **1978**, *100*, 6111.

(13) Yokoyama, A.; Ohba, H.; Hashimoto, M.; Katsumata, K.; Akagi, H.; Ishii, T.; Ohya, A.; Arai, S. *Appl. Phys. B* **2004**, *79*, 883.

(14) Hackett, P. A.; Gauthier, M.; Willis, C.; Pilon, R. *J. Chem. Phys.* **1979**, *71*, 546.

(15) Gauthier, M.; Nip, W. S.; Hackett, P. A.; Willis, C. *Chem. Phys. Lett.* **1980**, *69*, 372.

(16) Doljikov, V. S.; Kolomisky, Yu. R.; Ryabov, E. A. *Chem. Phys. Lett.* **1981**, *80*, 433.

(17) Gauthier, M.; Cureton, C. G.; Hackett, P. A.; Willis, C. *Appl. Phys. B* **1982**, *28*, 43.

(18) Frisch, M. J.; Trucks, G. W.; Schlegel, H. B.; Scuseria, G. E.; Robb, M. A.; Cheeseman, J. R.; Montgomery, J. A., Jr.; Vreven, T.; Kudin, K. N.; Burant, J. C.; Millam, J. M.; Iyengar, S. S.; Tomasi, J.; Barone, V.; Mennucci, B.; Cossi, M.; Scalmani, G.; Rega, N.; Petersson, G. A.; Nakatsuji, H.; Hada, M.; Ehara, M.; Toyota, K.; Fukuda, R.; Hasegawa, J.; Ishida, M.; Nakajima, T.; Honda, Y.; Kitao, O.; Nakai, H.; Klene, M.; Li, X.; Knox, J. E.; Hratchian, H. P.; Cross, J. B.; Adamo, C.; Jaramillo, J.; Gomperts, R.; Stratmann, R. E.; Yazyev, O.; Austin, A. J.; Cammi, R.; Pomelli, C.; Ochterski, J. W.; Ayala, P. Y.; Morokuma, K.; Voth, G. A.; Salvador, P.; Dannenberg, J. J.; Zakrzewski, V. G.; Dapprich, S.; Daniels, A. D.; Strain, M. C.; Farkas, O.; Malick, D. K.; Rabuck, A. D.; Raghavachari, K.; Foresman, J. B.; Ortiz, J. V.; Cui, Q.; Baboul, A. G.; Clifford, S.; Cioslowski, J.; Stefanov, B. B.; Liu, G.; Liashenko, A.; Piskorz, P.; Komaromi, I.; Martin, R. L.; Fox, D. J.; Keith, T.; Al-Laham, M. A.; Peng, C. Y.; Nanayakkara, A.; Challacombe, M.; Gill, P. M. W.; Johnson, B.; Chen, W.; Wong, M. W.; Gonzalez, C.; Pople, J. A. *Gaussian 03, Revision B.04, Gaussian, Inc., Pittsburgh PA* **2003**,

(19) Danen, W. C.; Jang, J. C. In *Laser Induced Chemical Processes*; Steinfeld, J. I., Ed.; Plenum: New York, 1981.

(20) Toselli, B.; Ferrero, J. C.; Staricco, E. H. J. *Phys. Chem.* **1986**, *90*, 4562.

(21) Azcárate, M. L.; Quel, E. J. J. *Phys. Chem.* **1989**, *93*, 697.

(22) Lide, D. R., Ed. *CRC Handbook of Chemistry and Physics* , 74th ed.; CRC Press: Boca Raton, FL, 1993.

(23) Holbrook, K. A.; Pilling, M. J.; Robertsonm S. H. *Unimolecular Reactions*, 2nd ed.; John Wiley & Sons: Chichester, 1996.

(24) Retzloff, D. G.; Coull, B. M.; Coull, J. *J. Phys. Chem.* **1970**, *74*, 2455.

(25) Garcia, D.; Grunwald, E. *J. Am. Chem. Soc.* **1980**, *102*, 6407.

(26) Boyarkin, O. V.; Kowalczyk, M.; Rizzo, T. R. *J. Chem. Phys.* **2003**, *118*, 93.

(27) Vagratashvili, V. N.; Letokhov, V. S.; Makarov, A. A.; Ryabov, E. A. *Laser Chem.* **1984**, *4*, 311.

JP802101H